

Origin of the superconducting state in the collapsed tetragonal phase of KFe_2As_2

Daniel Guterding,^{*} Steffen Backes, Harald O. Jeschke, and Roser Valentí

Institut für Theoretische Physik, Goethe-Universität Frankfurt, Max-von-Laue-Straße 1, 60438 Frankfurt am Main, Germany

(Received 21 January 2015; revised manuscript received 13 March 2015; published 13 April 2015)

Recently, KFe_2As_2 was shown to exhibit a structural phase transition from a tetragonal to a collapsed tetragonal phase under an applied pressure of about 15 GPa. Surprisingly, the collapsed tetragonal phase hosts a superconducting state with $T_c \sim 12$ K, while the tetragonal phase is a $T_c \leq 3.4$ K superconductor. We show that the key difference between the previously known nonsuperconducting collapsed tetragonal phase in $A\text{Fe}_2\text{As}_2$ ($A = \text{Ba}, \text{Ca}, \text{Eu}, \text{Sr}$) and the superconducting collapsed tetragonal phase in KFe_2As_2 is the qualitatively distinct electronic structure. While the collapsed phase in the former compounds features only electron pockets at the Brillouin zone boundary and no hole pockets are present in the Brillouin zone center, the collapsed phase in KFe_2As_2 has almost nested electron and hole pockets. Within a random phase approximation spin fluctuation approach we calculate the superconducting order parameter in the collapsed tetragonal phase. We propose that a Lifshitz transition associated with the structural collapse changes the pairing symmetry from d wave (tetragonal) to s_{\pm} (collapsed tetragonal). Our density functional theory combined with dynamical mean-field theory calculations show that effects of correlations on the electronic structure of the collapsed tetragonal phase are minimal. Finally, we argue that our results are compatible with a change of sign of the Hall coefficient with pressure, as observed experimentally.

DOI: 10.1103/PhysRevB.91.140503

PACS number(s): 71.15.Mb, 71.18.+y, 74.20.Pq, 74.70.Xa

The family of $A\text{Fe}_2\text{As}_2$ ($A = \text{Ba}, \text{Ca}, \text{Eu}, \text{K}, \text{Sr}$) superconductors, also called 122 materials, has been intensively investigated in the past due to its richness in structural, magnetic, and superconducting phases upon doping or application of pressure [1–6]. One phase whose properties have been recently scrutinized at length is the collapsed tetragonal (CT) phase present in BaFe_2As_2 , CaFe_2As_2 , EuFe_2As_2 , and SrFe_2As_2 under pressure, and in CaFe_2P_2 [7–14]. The structural collapse of this phase has been shown to be assisted by the formation of As $4p_z$ -As $4p_z$ bonds between adjacent Fe-As layers, giving rise to a bonding-antibonding splitting of the As p_z bands [15]. It has been argued that this phase does not support superconductivity due to the absence of hole cylinders at the Brillouin zone center and the corresponding suppression of spin fluctuations [10,16,17]. However, recently Ying *et al.* [18] investigated the hole-doped end member of $\text{Ba}_{1-x}\text{K}_x\text{Fe}_2\text{As}_2$, KFe_2As_2 , under high pressure and observed a boost of the superconducting critical temperature T_c up to 12 K, precisely when the system undergoes a structural phase transition to a CT phase at a pressure $P_c \sim 15$ GPa. These authors attributed this behavior to possible correlation effects. Moreover, measurements of the Hall coefficient showed a change from positive to negative sign upon pressure, indicating that the effective nature of charge carriers changes from holes to electrons with increasing pressure. Similar experiments are also reported in Ref. [19].

KFe_2As_2 has a few distinct features: At ambient pressure, the system shows superconductivity at $T_c = 3.4$ K and follows a V-shaped pressure dependence of T_c for moderate pressures with a local minimum at a pressure of 1.55 GPa [20]. The origin of such behavior and the nature of the superconducting pairing symmetry are still under debate [21–27]. However, it has been established by a few experimental and theoretical

investigations based on angle-resolved photoemission spectroscopy, de Haas-van Alphen measurements, and density functional theory combined with dynamical mean-field theory (DFT+DMFT) calculations that correlation effects crucially influence the behavior of this system at $P = 0$ GPa [28–35]. Application of pressure should nevertheless reduce the relative importance of correlations with respect to the bandwidth increase. In fact, recent DFT+DMFT studies on CaFe_2As_2 in the high-pressure CT phase show that the topology of the Fermi surface is basically unaffected by correlations [36,37]. One could argue, though, that at ambient pressure CaFe_2As_2 is less correlated than KFe_2As_2 , and therefore in KFe_2As_2 correlation effects may be still significant at finite pressure.

In order to resolve these questions, we performed density functional theory (DFT) as well as DFT+DMFT calculations for KFe_2As_2 in the CT phase. Our results show that the origin of superconductivity in the collapsed tetragonal phase in KFe_2As_2 lies in the qualitative changes in the electronic structure (Lifshitz transition) experienced under compression to a collapsed tetragonal phase, and correlations play only a minor role. Whereas in the tetragonal phase at $P = 0$ GPa, KFe_2As_2 features predominantly only hole pockets at the Brillouin zone center, at $P \sim 15$ GPa, in the CT phase, significant electron pockets emerge at the Brillouin zone boundary, which, together with the hole pockets at the Brillouin zone center, favor a superconducting state with s_{\pm} symmetry, as we show in our calculations of the superconducting gap function using the random phase approximation (RPA) spin fluctuation approach. Moreover, our results in the tetragonal phase of KFe_2As_2 at $P = 10$ GPa suggest a change of pairing symmetry from d_{xy} (tetragonal) to s_{\pm} upon entering the collapsed phase (see Fig. 1). This scenario is distinct from the physics of the CT phase in CaFe_2As_2 , where the hole pockets at the Brillouin zone center are absent. For comparison, we will present the susceptibility of collapsed tetragonal CaFe_2As_2 , which is representative for the collapsed phase of $A\text{Fe}_2\text{As}_2$ ($A = \text{Ba}, \text{Ca}, \text{Eu}, \text{Sr}$). Our findings also suggest an explanation

*guterding@itp.uni-frankfurt.de

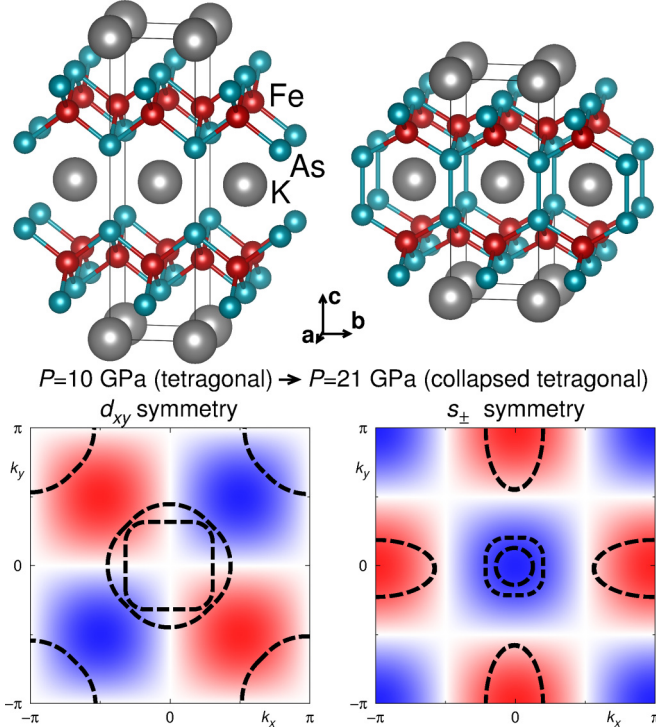


FIG. 1. (Color online) Crystal structure, schematic Fermi surface (dashed lines), and schematic superconducting gap function (background color) of KFe₂As₂ in the one-Fe Brillouin zone before and after the volume collapse. The Lifshitz transition associated with the formation of As 4p_z-As 4p_z bonds in the CT phase changes the superconducting pairing symmetry from d_{xy} to s_{\pm} .

for the change of sign in the Hall coefficient upon entering the CT phase in KFe₂As₂.

Density functional theory calculations were carried out using the all-electron full-potential local orbital (FPLO) [38] code. For the exchange-correlation functional we use the generalized gradient approximation (GGA) by Perdew, Burke, and Ernzerhof [39]. All calculations were converged on $20 \times 20 \times 20$ k -point grids.

The structural parameters for the CT phase of KFe₂As₂ were taken from Ref. [18]. We used the data points at $P \approx 21$ GPa, deep in the CT phase, where $a = 3.854$ Å and $c = 9.6$ Å. The fractional arsenic z position ($z_{\text{As}} = 0.36795$) was determined *ab initio* via structural relaxation using the FPLO code. We also performed calculations for the crystal structure of Ref. [19], where a preliminary experimental value for the arsenic z position was given. The electronic structure is very similar to the one reported here. For the CT phase of CaFe₂As₂ we used experimental lattice parameters from Ref. [40] ($T = 40$ K, $P \approx 21$ GPa) and determined the fractional arsenic z position ($z_{\text{As}} = 0.37045$) using FPLO. All Fe 3d orbitals are defined in a coordinate system rotated by 45° around the z axis with respect to the conventional $I4/mmm$ unit cell.

The electronic band structure in the collapsed tetragonal phase of CaFe₂As₂ and KFe₂As₂ is shown in Fig. 2. These results already reveal a striking difference between the CT phases of CaFe₂As₂ and KFe₂As₂: While the former does not feature hole bands crossing the Fermi level at Γ and only one band crossing the Fermi level at $M(\pi, \pi, 0)$, the latter does

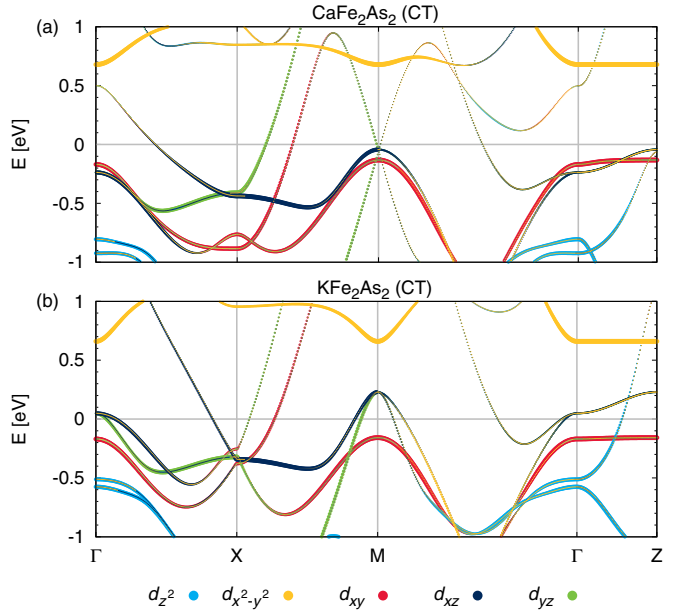


FIG. 2. (Color online) Electronic band structure of the collapsed tetragonal phase in (a) CaFe₂As₂ and (b) KFe₂As₂. The path is chosen in the one-Fe equivalent Brillouin zone. The colors indicate the weights of Fe 3d states.

feature hole pockets at both Γ and M in the one-Fe equivalent Brillouin zone. The reason for this difference in electronic structure is that KFe₂As₂ is strongly hole doped compared to CaFe₂As₂.

In Fig. 3 we show the Fermi surface in the one-Fe equivalent Brillouin zone at $k_z = 0$. In both cases, the Fermi surface is dominated by Fe 3d_{xz/yz} character. The hole cylinders in KFe₂As₂ span the entire k_z direction of the Brillouin zone, while only a small three-dimensional hole pocket is present in CaFe₂As₂ (see Ref. [41]). For KFe₂As₂, the hole pockets at $M(\pi, \pi, 0)$ and the electron pockets at $X(\pi, 0, 0)$ are clearly nested, while no nesting is observed for CaFe₂As₂. It is important to note here that the folding vector in the 122 family of iron-based superconductors is (π, π, π) , so that the

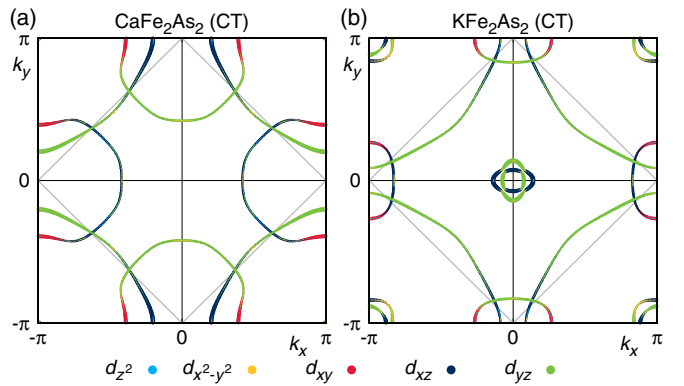


FIG. 3. (Color online) Fermi surface of the collapsed tetragonal phase in (a) CaFe₂As₂ and (b) KFe₂As₂ at $k_z = 0$. The full plot spans the one-Fe equivalent Brillouin zone, while the area enclosed by the gray lines is the two-Fe equivalent Brillouin zone. The colors indicate the weights of Fe 3d states.

hole pockets at $M(\pi, \pi, 0)$ will be located at $Z(0, 0, \pi)$ after unfolding the bands to the effective one-Fe picture [42].

After qualitatively identifying the difference between the CT phases of CaFe_2As_2 and KFe_2As_2 , we calculate the non-interacting static susceptibility to verify that the better nesting of KFe_2As_2 generates stronger spin fluctuations. For that we constructed 16-band tight-binding models from the DFT results using projective Wannier functions as implemented in FPLO [43]. We keep the Fe $3d$ and As $4p$ states, which corresponds to an energy window from -7 to $+6$ eV. Subsequently, we unfold the 16-band model using our recently developed glide reflection unfolding technique [42], which produces an effective eight-band model of the three-dimensional one-Fe Brillouin zone.

We analyze these eight-band models using the three-dimensional (3D) version of random phase approximation (RPA) spin fluctuation theory [44] with a Hamiltonian $H = H_0 + H_{\text{int}}$, where H_0 is the eight-band tight-binding Hamiltonian derived from the *ab initio* calculations, while H_{int} is the Hubbard-Hund interaction. The arsenic states are kept in the entire calculation, but interactions are considered only between Fe $3d$ states. Further information is given in Ref. [41].

The noninteracting static susceptibility in orbital space is defined by Eq. (1), where matrix elements $a_{\mu}^s(\vec{k})$ resulting from the diagonalization of the initial Hamiltonian H_0 connect orbital and band space denoted by indices s and μ , respectively. The E_{μ} are the eigenvalues of H_0 and $f(E)$ is the Fermi function:

$$\chi_{st}^{pq}(\vec{q}) = -\frac{1}{N} \sum_{\vec{k}, \mu, v} a_{\mu}^s(\vec{k}) a_{\mu}^{p*}(\vec{k}) a_v^q(\vec{k} + \vec{q}) a_v^{t*}(\vec{k} + \vec{q}) \times \frac{f(E_v(\vec{k} + \vec{q})) - f(E_{\mu}(\vec{k}))}{E_v(\vec{k} + \vec{q}) - E_{\mu}(\vec{k})} \quad (1)$$

The observable static susceptibility [41] is defined as the sum over all elements χ_{aa}^{bb} of the full tensor $\chi(\vec{q}) = \frac{1}{2} \sum_{a,b} \chi_{aa}^{bb}(\vec{q})$.

The effective interaction in the singlet pairing channel is constructed from the static susceptibility tensor χ_{st}^{pq} which measures strength and wave-vector dependence of spin fluctuations, via the multiorbital RPA procedure. Both the original and effective interaction are discussed, e.g., in Ref. [45]. We have shown previously that our implementation is capable of capturing the effects of fine variations of shape and orbital character of the Fermi surface [46].

At first glance, the observable static susceptibility displayed in Fig. 4 is comparable for CaFe_2As_2 and KFe_2As_2 . A key difference is, however, revealed upon investigation of the largest elements, i.e., the diagonal entries χ_{aa}^{aa} . These show that in CaFe_2As_2 the susceptibility has broad plateaus, while in KFe_2As_2 the susceptibility has a strong peak at $X(\pi, 0, 0)$ in the one-Fe Brillouin zone, which corresponds to the usual s_{\pm} pairing scenario that relies on electron-hole nesting. In CaFe_2As_2 the pairing interaction is highly frustrated because there is no clear peak in favor of one pairing channel.

We have also performed spin-polarized calculations for KFe_2As_2 at $P \approx 21$ GPa in order to confirm the antiferromagnetic instability we find in the linear response calculations. Out of ferromagnetic, Néel, and stripe antiferromagnetic order, only the stripe antiferromagnet is stable with small moments

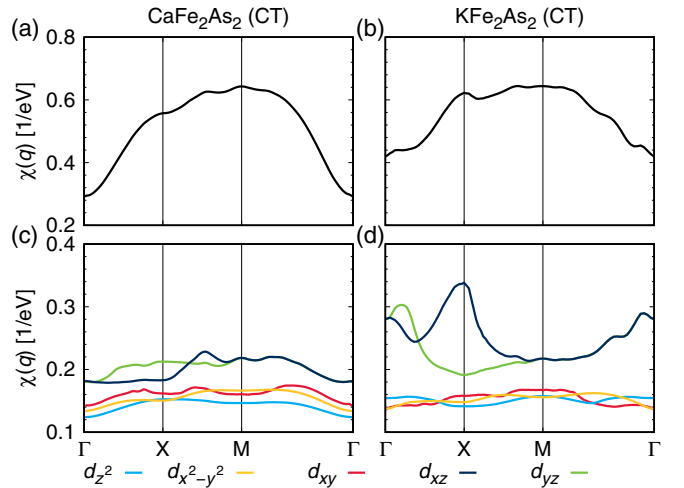


FIG. 4. (Color online) Summed static susceptibility (top) and its diagonal components χ_{aa}^{aa} (bottom) in the eight-band tight-binding model for (a), (c) CaFe_2As_2 and (b), (d) KFe_2As_2 in the one-Fe Brillouin zone. The colors identify the Fe $3d$ states.

of $0.07\mu_B$ on Fe, in agreement with our calculations for the susceptibility.

The leading superconducting gap function of KFe_2As_2 in the CT phase is shown in Fig. 5. As expected from our susceptibility calculations, the pairing symmetry is s wave with a sign change between electron and hole pockets. While the superconducting gap is nodeless in the $k_z = 0$ plane, the $k_z = \pi$ plane does show nodes where the orbital character changes from Fe $3d_{xz/yz}$ to Fe $3d_{xy}$. Note that this $k_z = \pi$ structure of the superconducting gap is exactly the same as in the well-studied LaFeAsO compound [44], which shows that the CT phase of KFe_2As_2 closely resembles usual iron-based superconductors, although it is much more three dimensional than, e.g., in LaFeAsO .

We have also calculated the superconducting gap function for KFe_2As_2 at $P = 10$ GPa in the tetragonal phase and find d_{xy} as the leading pairing symmetry [41]. The dominant $d_{x^2-y^2}$ solution obtained in model calculations based on rigid band shifts [22,24] is also present in our calculation, but as a subleading solution. Our results strongly suggest that the Lifshitz transition, which occurs upon entering the

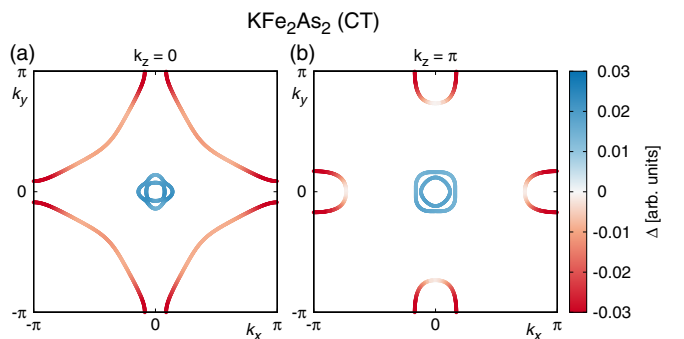


FIG. 5. (Color online) Leading superconducting gap function (s_{\pm}) of the eight-band model in the one-Fe Brillouin zone of KFe_2As_2 in the CT phase at (a) $k_z = 0$ and (b) $k_z = \pi$.

TABLE I. Mass renormalizations m^*/m_{LDA} of the Fe $3d$ orbitals in the collapsed tetragonal phase of KFe_2As_2 calculated with the LDA+DMFT method.

d_{z^2}	$d_{x^2-y^2}$	d_{xy}	$d_{xz/yz}$
1.318	1.309	1.319	1.445

collapsed tetragonal phase, changes the symmetry of the superconducting gap function from d wave (tetragonal) to s wave (CT) (see Fig. 1). The possible simultaneous change of pairing symmetry, density of states, and T_c potentially opens up different routes to understanding their quantitative connection.

In order to estimate the strength of local electronic correlations in collapsed tetragonal KFe_2As_2 , we performed fully charge self-consistent DFT+DMFT calculations. We used the same method as described in Ref. [35]. The DFT calculation was performed by the WIEN2K [47] implementation of the full-potential linear augmented plane wave (FLAPW) method in the local density approximation (LDA) with 726 k points in the irreducible Brillouin zone. We checked that the results of FPLO and WIEN2K agree on the DFT level. The Bloch wave functions are projected to the localized Fe $3d$ orbitals, as described in Refs. [48,49]. The energy window for projection was chosen from -7 to $+13$ eV, with the lower boundary lying in a gap in the density of states. For the solution of the DMFT impurity problem, the continuous-time quantum Monte Carlo method in the hybridization expansion [50] as implemented in the ALPS [51,52] project was employed (see Ref. [41] for more details). The mass renormalizations are directly calculated from the analytically continued real part of the impurity self-energy $\Sigma(\omega)$ via $\frac{m^*}{m_{\text{LDA}}} = 1 - \frac{\partial \text{Re } \Sigma(\omega)}{\partial \omega} |_{\omega \rightarrow 0}$.

Table I displays the orbital-resolved mass renormalizations m^*/m_{LDA} for KFe_2As_2 in the collapsed tetragonal phase. The obtained values show that local electronic correlations in the CT phases of KFe_2As_2 and CaFe_2As_2 [36,37] are comparable. As in CaFe_2As_2 , the effects of local electronic correlations on the Fermi surface are negligible (see Ref. [41]). The higher

T_c of the collapsed phase in the absence of strong correlations raises the question of how important strong correlations are in general for iron-based superconductivity. This issue demands further investigation.

Finally, the change of dominant charge carriers from hole to electronlike states measured in the Hall coefficient under pressure [18] is naturally explained from our calculated Fermi surfaces. While KFe_2As_2 is known to show only hole pockets at zero pressure, the CT phase features also large electron pockets. On a small fraction of these electron pockets, the dominating orbital character is Fe $3d_{xy}$ (Fig. 3). It was shown in Ref. [53] that quasiparticle lifetimes on the Fermi surface can be very anisotropic and long-lived states are favored where marginal orbital characters appear. As Fe $3d_{xy}$ character is only present on the electron pockets, these states contribute significantly to transport and are responsible for the negative sign of the Hall coefficient.

In summary, we have shown that the electronic structure of the collapsed tetragonal phase of KFe_2As_2 qualitatively differs from that of other known collapsed materials. Upon entering the CT phase, the Fermi surface of KFe_2As_2 undergoes a Lifshitz transition with electron pockets appearing at the Brillouin zone boundary, which are nested with the hole pockets at the Brillouin zone center. Thus, the spin fluctuations in collapsed tetragonal KFe_2As_2 resemble those of other iron-based superconductors in noncollapsed phases, and the superconducting gap function assumes the well-known s_{\pm} symmetry. This is in contrast to other known materials in the CT phase, such as CaFe_2As_2 , where hole pockets at the Brillouin zone center are absent and no superconductivity is favored. Based on our LDA+DMFT calculations, the CT phase of KFe_2As_2 is significantly less correlated than the tetragonal phase, and mass enhancements are comparable to the CT phase of CaFe_2As_2 . Finally, we suggest that the change of dominant charge carriers from hole to electronlike can be explained from anisotropic quasiparticle lifetimes.

We thank the Deutsche Forschungsgemeinschaft for financial support through Grant No. SPP 1458.

-
- [1] M. Rotter, M. Tegel, and D. Johrendt, Superconductivity at 38 K in the iron arsenide $(\text{Ba}_{1-x}\text{K}_x)\text{Fe}_2\text{As}_2$, *Phys. Rev. Lett.* **101**, 107006 (2008).
 - [2] S. A. J. Kimber, A. Kreyssig, Y. Z. Zhang, H. O. Jeschke, R. Valentí, F. Yokaichiya, E. Colombier, J. Yan, T. C. Hansen, T. Chatterji, R. J. McQueeney, P. C. Canfield, A. I. Goldman, and D. N. Argyriou, Similarities between structural distortions under pressure and chemical doping in superconducting BaFe_2As_2 , *Nat. Mater.* **8**, 471 (2009).
 - [3] J. Paglione and R. L. Greene, High-temperature superconductivity in iron-based materials, *Nat. Phys.* **6**, 645 (2010).
 - [4] E. Gati, S. Köhler, D. Guterding, B. Wolf, S. Knöner, S. Ran, S. L. Bud'ko, P. C. Canfield, and M. Lang, Hydrostatic-pressure tuning of magnetic, nonmagnetic, and superconducting states in annealed $\text{Ca}(\text{Fe}_{1-x}\text{Co}_x)_2\text{As}_2$, *Phys. Rev. B* **86**, 220511(R) (2012).
 - [5] S. Lee, J. Jiang, Y. Zhang, C. W. Bark, J. D. Weiss, C. Tarantini, C. T. Nelson, H. W. Jang, C. M. Folkman, S. H. Baek, A. Polyanskii, D. Abraimov, A. Yamamoto, J. W. Park, X. Q. Pan, E. E. Hellstrom, D. C. Larbalestier, and C. B. Eom, Template engineering of Co-doped BaFe_2As_2 single-crystal thin films, *Nat. Mater.* **9**, 397 (2010).
 - [6] A. Leithe-Jasper, W. Schnelle, C. Geibel, and H. Rosner, Superconducting State in $\text{SrFe}_{2-x}\text{Co}_x\text{As}_2$ by internal doping of the iron arsenide layers, *Phys. Rev. Lett.* **101**, 207004 (2008).
 - [7] W. Uhoya, A. Stemshorn, G. Tsui, Y. K. Vohra, A. S. Sefat, B. C. Sales, K. M. Hope, and S. T. Weir, Collapsed tetragonal phase and superconductivity of BaFe_2As_2 under high pressure, *Phys. Rev. B* **82**, 144118 (2010).
 - [8] N. Ni, S. Nandi, A. Kreyssig, A. I. Goldman, E. D. Mun, S. L. Bud'ko, and P. C. Canfield, First-order structural phase transition in CaFe_2As_2 , *Phys. Rev. B* **78**, 014523 (2008).

- [9] Y.-Z. Zhang, H. C. Kandpal, I. Opahle, H. O. Jeschke, and R. Valentí, Microscopic origin of pressure-induced phase transitions in the iron pnictide superconductors AFe_2As_2 : An *ab initio* molecular dynamics study, *Phys. Rev. B* **80**, 094530 (2009).
- [10] R. S. Dhaka, R. Jiang, S. Ran, S. L. Bud'ko, P. C. Canfield, B. N. Harmon, A. Kaminski, M. Tomic, R. Valentí, and Y. Lee, Dramatic changes in the electronic structure upon transition to the collapsed tetragonal phase in $CaFe_2As_2$, *Phys. Rev. B* **89**, 020511(R) (2014).
- [11] D. Kasinathan, M. Schmitt, K. Koepernik, A. Ormeci, K. Meier, U. Schwarz, M. Hanfland, C. Geibel, Y. Grin, A. Leithe-Jasper, and H. Rosner, Symmetry-preserving lattice collapse in tetragonal $SrFe_{2-x}Ru_xAs_2$ ($x = 0, 0.2$): A combined experimental and theoretical study, *Phys. Rev. B* **84**, 054509 (2011).
- [12] W. Uhoya, G. Tsoi, Y. K. Vohra, M. A. McGuire, A. S. Sefat, B. C. Sales, D. Mandrus, and S. T. Weir, Anomalous compressibility effects and superconductivity of $EuFe_2As_2$ under high pressures, *J. Phys.: Condens. Matter* **22**, 292202 (2010).
- [13] A. I. Coldea, C. M. J. Andrew, J. G. Analytis, R. D. McDonald, A. F. Bangura, J.-H. Chu, I. R. Fisher, and A. Carrington, Topological change of the Fermi surface in ternary iron pnictides with reduced c/a ratio: A de Haas–van Alphen study of $CaFe_2P_2$, *Phys. Rev. Lett.* **103**, 026404 (2009).
- [14] N. Colonna, G. Profeta, A. Continenza, and S. Massidda, Structural and magnetic properties of $CaFe_2As_2$ and $BaFe_2As_2$ from first-principles density functional theory, *Phys. Rev. B* **83**, 094529 (2011).
- [15] T. Yildirim, Strong coupling of the Fe-Spin state and the As-As hybridization in iron-pnictide superconductors from first-principle calculations, *Phys. Rev. Lett.* **102**, 037003 (2009).
- [16] D. K. Pratt, Y. Zhao, S. A. J. Kimber, A. Hiess, D. N. Argyriou, C. Broholm, A. Kreyssig, S. Nandi, S. L. Bud'ko, N. Ni, P. C. Canfield, R. J. McQueeney, and A. I. Goldman, Suppression of antiferromagnetic spin fluctuations in the collapsed phase of $CaFe_2As_2$, *Phys. Rev. B* **79**, 060510(R) (2009).
- [17] J. H. Soh, G. S. Tucker, D. K. Pratt, D. L. Abernathy, M. B. Stone, S. Ran, S. L. Bud'ko, P. C. Canfield, A. Kreyssig, R. J. McQueeney, and A. I. Goldman, Inelastic neutron scattering study of a nonmagnetic collapsed tetragonal phase in nonsuperconducting $CaFe_2As_2$: Evidence of the impact of spin fluctuations on superconductivity in the iron-arsenide compounds, *Phys. Rev. Lett.* **111**, 227002 (2013).
- [18] J.-J. Ying, L.-Y. Tang, V. V. Struzhkin, H.-K. Mao, A. G. Gavriluk, A.-F. Wang, X.-H. Chen, and X.-J. Chen, *arXiv:1501.00330*.
- [19] Y. Nakajima, R. Wang, T. Metz, X. Wang, L. Wang, H. Cynn, S. T. Weir, J. R. Jeffries, and J. Paglione, High-temperature superconductivity stabilized by electron-hole interband coupling in collapsed tetragonal phase of KFe_2As_2 under high pressure, *Phys. Rev. B* **91**, 060508(R) (2015).
- [20] F. F. Tafti, A. Juneau-Fecteau, M.-È. Delage, S. René de Cotret, J.-Ph. Reid, A. F. Wang, X-G. Luo, X. H. Chen, N. Doiron-Leyraud, and L. Taillefer, Sudden reversal in the pressure dependence of T_c in the iron-based superconductor KFe_2As_2 , *Nat. Phys.* **9**, 349 (2013).
- [21] K. Okazaki, Y. Ota, Y. Kotani, W. Malaeb, Y. Ishida, T. Shimojima, T. Kiss, S. Watanabe, C.-T. Chen, K. Kihou, C.-H. Lee, A. Iyo, H. Eisaki, T. Saito, H. Fukazawa, Y. Kohori, K. Hashimoto, T. Shibauchi, Y. Matsuda, H. Ikeda, H. Miyahara, R. Arita, A. Chainani, and S. Shin, Octet-line node structure of superconducting order parameter in KFe_2As_2 , *Science* **337**, 1314 (2012).
- [22] R. Thomale, Ch. Platt, W. Hanke, J. Hu, and B. A. Bernevig, Exotic d -wave superconducting state of strongly hole-doped $K_xBa_{1-x}Fe_2As_2$, *Phys. Rev. Lett.* **107**, 117001 (2011).
- [23] J.-Ph. Reid, M. A. Tanatar, A. Juneau-Fecteau, R. T. Gordon, S. René de Cotret, N. Doiron-Leyraud, T. Saito, H. Fukazawa, Y. Kohori, K. Kihou, C.-H. Lee, A. Iyo, H. Eisaki, R. Prozorov, and L. Taillefer, Universal heat conduction in the iron arsenide superconductor KFe_2As_2 : Evidence of a d -wave state, *Phys. Rev. Lett.* **109**, 087001 (2012).
- [24] S. Maiti, M. M. Korshunov, T. A. Maier, P. J. Hirschfeld, and A. V. Chubukov, Evolution of the superconducting state of Fe-based compounds with doping, *Phys. Rev. Lett.* **107**, 147002 (2011).
- [25] K. Suzuki, H. Usui, and K. Kuroki, Spin fluctuations and unconventional pairing in KFe_2As_2 , *Phys. Rev. B* **84**, 144514 (2011).
- [26] F. F. Tafti, J. P. Clancy, M. Lapointe-Major, C. Collignon, S. Faucher, J. A. Sears, A. Juneau-Fecteau, N. Doiron-Leyraud, A. F. Wang, X.-G. Luo, X. H. Chen, S. Desgreniers, Y.-J. Kim, and L. Taillefer, Sudden reversal in the pressure dependence of T_c in the iron-based superconductor $CsFe_2As_2$: A possible link between inelastic scattering and pairing symmetry, *Phys. Rev. B* **89**, 134502 (2014).
- [27] F. F. Tafti, A. Ouellet, A. Juneau-Fecteau, S. Faucher, M. Lapointe-Major, N. Doiron-Leyraud, A. F. Wang, X. G. Luo, X. H. Chen, and L. Taillefer, Universal V-shaped temperature-pressure phase diagram in the iron-based superconductors KFe_2As_2 , $RbFe_2As_2$, and $CsFe_2As_2$, *Phys. Rev. B* **91**, 054511 (2015).
- [28] T. Terashima, M. Kimata, N. Kurita, H. Satsukawa, A. Harada, K. Hazama, M. Imai, A. Sato, K. Kihou, C.-H. Lee, H. Kito, H. Eisaki, A. Iyo, T. Saito, H. Fukazawa, Y. Kohori, H. Harima, and S. Uji, Fermi surface and mass enhancements in KFe_2As_2 from de Haas–van Alphen effect measurements, *J. Phys. Soc. Jpn.* **79**, 053702 (2010).
- [29] T. Yoshida, I. Nishi, A. Fujimori, M. Yi, R. G. Moore, D.-H. Lu, Z.-X. Shen, K. Kihou, P. M. Shirage, H. Kito, C.-H. Lee, A. Iyo, H. Eisaki, and H. Harima, Fermi surfaces and quasi-particle band dispersions of the iron pnictide superconductor KFe_2As_2 observed by angle-resolved photoemission spectroscopy, *J. Phys. Chem. Solids* **72**, 465 (2011).
- [30] M. Kimata, T. Terashima, N. Kurita, H. Satsukawa, A. Harada, K. Kodama, K. Takehana, Y. Imanaka, T. Takamasu, K. Kihou, C.-H. Lee, H. Kito, H. Eisaki, A. Iyo, H. Fukazawa, Y. Kohori, H. Harima, and S. Uji, Cyclotron resonance and mass enhancement by electron correlation in KFe_2As_2 , *Phys. Rev. Lett.* **107**, 166402 (2011).
- [31] T. Sato, N. Nakayama, Y. Sekiba, P. Richard, Y.-M. Xu, S. Souma, T. Takahashi, G. F. Chen, J. L. Luo, N. L. Wang, and H. Ding, Band structure and Fermi surface of an extremely overdoped iron-based superconductor KFe_2As_2 , *Phys. Rev. Lett.* **103**, 047002 (2009).
- [32] T. Yoshida, S. Ideta, I. Nishi, A. Fujimori, M. Yi, R. G. Moore, S. K. Mo, D.-H. Lu, Z-X. Shen, Z. Hussain, K. Kihou, P. M. Shirage, H. Kito, C.-H. Lee, A. Iyo, H. Eisaki, and H. Harima, Orbital character and electron correlation effects on two- and three-dimensional Fermi surfaces in KFe_2As_2 revealed by angle-resolved photoemission spectroscopy, *Front. Phys.* **2**, 17 (2014).

- [33] T. Terashima, N. Kurita, M. Kimata, M. Tomita, S. Tsuchiya, M. Imai, A. Sato, K. Kihou, C-H. Lee, H. Kito, H. Eisaki, A. Iyo, T. Saito, H. Fukazawa, Y. Kohori, H. Harima, and S. Uji, Fermi surface in KFe_2As_2 determined via de Haas–van Alphen oscillation measurements, *Phys. Rev. B* **87**, 224512 (2013).
- [34] Z. P. Yin, K. Haule, and G. Kotliar, Kinetic frustration and the nature of the magnetic and paramagnetic states in iron pnictides and iron chalcogenides, *Nat. Mater.* **10**, 932 (2011).
- [35] S. Backes, D. Guterding, H. O. Jeschke, and R. Valentí, Electronic structure and de Haas–van Alphen frequencies in KFe_2As_2 within LDA+DMFT, *New J. Phys.* **16**, 083025 (2014).
- [36] S. Mandal, R. E. Cohen, and K. Haule, Pressure suppression of electron correlation in the collapsed tetragonal phase of $CaFe_2As_2$: A DFT-DMFT investigation, *Phys. Rev. B* **90**, 060501(R) (2014).
- [37] J. Diehl, S. Backes, D. Guterding, H. O. Jeschke, and R. Valentí, Correlation effects in the tetragonal and collapsed tetragonal phase of $CaFe_2As_2$, *Phys. Rev. B* **90**, 085110 (2014).
- [38] K. Koepernik and H. Eschrig, Full-potential nonorthogonal local-orbital minimum-basis band-structure scheme, *Phys. Rev. B* **59**, 1743 (1999); <http://www.FPLO.de>.
- [39] J. P. Perdew, K. Burke, and M. Ernzerhof, Generalized gradient approximation made simple, *Phys. Rev. Lett.* **77**, 3865 (1996).
- [40] R. Mittal, S. K. Mishra, S. L. Chaplot, S. V. Ovsyannikov, E. Greenberg, D. M. Trots, L. Dubrovinsky, Y. Su, Th. Bruckel, S. Matsuishi, H. Hosono, and G. Garbarino, Ambient- and low-temperature synchrotron x-ray diffraction study of $BaFe_2As_2$ and $CaFe_2As_2$ at high pressures up to 56 GPa, *Phys. Rev. B* **83**, 054503 (2011).
- [41] See Supplemental Material at <http://link.aps.org/supplemental/10.1103/PhysRevB.91.140503>, which includes further information on the tight-binding model construction, the RPA pairing calculations, three-dimensional Fermi surface plots, an electronic structure calculation for a high-pressure noncollapsed structure of KFe_2As_2 , and further details on the LDA+DMFT calculations outlined in the main text. For the latter we present momentum-resolved and momentum-integrated spectral functions and the Fermi surface.
- [42] M. Tomić, H. O. Jeschke, and R. Valentí, Unfolding of electronic structure through induced representations of space groups: Application to Fe-based superconductors, *Phys. Rev. B* **90**, 195121 (2014).
- [43] H. Eschrig and K. Koepernik, Tight-binding models for the iron-based superconductors, *Phys. Rev. B* **80**, 104503 (2009).
- [44] S. Graser, T. A. Maier, P. J. Hirschfeld, and D. J. Scalapino, Near-degeneracy of several pairing channels in multiorbital models for the Fe pnictides, *New J. Phys.* **11**, 025016 (2009).
- [45] P. J. Hirschfeld, M. M. Korshunov, and I. I. Mazin, Gap symmetry and structure of Fe-based superconductors, *Rep. Prog. Phys.* **74**, 124508 (2011).
- [46] D. Guterding, H. O. Jeschke, P. J. Hirschfeld, and R. Valentí, Unified picture of the doping dependence of superconducting transition temperatures in alkali metal/ammonia intercalated FeSe, *Phys. Rev. B* **91**, 041112(R) (2015).
- [47] P. Blaha, K. Schwarz, G. K. H. Madsen, D. Kvasnicka, and J. Luitz, *An Augmented Plane Wave Plus Local Orbitals Program for Calculating Crystal Properties* (Karlheinz Schwarz, Techn. Universität Wien, Austria, 2001).
- [48] M. Aichhorn, L. Pourovskii, V. Vildosola, M. Ferrero, O. Parcollet, T. Miyake, A. Georges, and S. Biermann, Dynamical mean-field theory within an augmented plane-wave framework: Assessing electronic correlations in the iron pnictide $LaFeAsO$, *Phys. Rev. B* **80**, 085101 (2009).
- [49] J. Ferber, K. Foyevtsova, H. O. Jeschke, and R. Valentí, Unveiling the microscopic nature of correlated organic conductors: The case of κ - $(ET)_2Cu[N(CN)_2]Br_xCl_{1-x}$, *Phys. Rev. B* **89**, 205106 (2014).
- [50] P. Werner, A. Comanac, L. de' Medici, M. Troyer, and A. J. Millis, Continuous-time solver for quantum impurity models, *Phys. Rev. Lett.* **97**, 076405 (2006).
- [51] B. Bauer, L. D. Carr, H. G. Evertz, A. Feiguin, J. Freire, S. Fuchs, L. Gamper, J. Gukelberger, E. Gull, S. Guertler *et al.*, The ALPS project release 2.0: Open source software for strongly correlated systems, *J. Stat. Mech.: Theory Exp.* (2011) P05001.
- [52] E. Gull, P. Werner, S. Fuchs, B. Surer, T. Pruschke, and M. Troyer, Continuous-time quantum Monte Carlo impurity solvers, *Comput. Phys. Commun.* **182**, 1078 (2011).
- [53] A. F. Kemper, M. M. Korshunov, T. P. Devreux, J. N. Fry, H.-P. Cheng, and P. J. Hirschfeld, Anisotropic quasiparticle lifetimes in Fe-based superconductors, *Phys. Rev. B* **83**, 184516 (2011).